

See discussions, stats, and author profiles for this publication at: <https://www.researchgate.net/publication/231700288>

# Synthesis, Characterization, Crystalline Morphologies, and Hydrophilicity of Brush Copolymers with Double Crystallizable Side Chains

ARTICLE in *MACROMOLECULES* · NOVEMBER 2007

Impact Factor: 5.8 · DOI: 10.1021/ma071841u

---

CITATIONS

66

---

READS

45

5 AUTHORS, INCLUDING:



Jinying Yuan

Tsinghua University

78 PUBLICATIONS 2,154 CITATIONS

SEE PROFILE



Fengbo Zhang

Capital Medical University

17 PUBLICATIONS 312 CITATIONS

SEE PROFILE



Xu-Ming Xie

Tsinghua University

168 PUBLICATIONS 1,590 CITATIONS

SEE PROFILE

# Synthesis, Characterization, Crystalline Morphologies, and Hydrophilicity of Brush Copolymers with Double Crystallizable Side Chains

Weizhong Yuan,<sup>†</sup> Jinying Yuan,<sup>\*,†</sup> Fengbo Zhang,<sup>‡</sup> Xuming Xie,<sup>‡</sup> and Caiyuan Pan<sup>§</sup>

Key Lab of Organic Optoelectronics & Molecular Engineering of Ministry of Education, Department of Chemistry, and Department of Chemical Engineering, Tsinghua University, Beijing 100084, People's Republic of China, and Department of Polymer Science and Engineering, University of Science and Technology of China, Hefei, Anhui 230026, People's Republic of China

Received August 14, 2007; Revised Manuscript Received September 24, 2007

**ABSTRACT:** Novel brush copolymers with poly(2-hydroxyethyl methacrylate) (PHEMA) as polymer backbone and diblock copolymer consisting of crystallizable poly( $\epsilon$ -caprolactone) (PCL) and poly(ethylene oxide) (PEO) as side chains were synthesized successively by the combination of ring-opening polymerization (ROP) and coupling reaction. The molecular weights of poly(2-hydroxyethyl methacrylate)-*graft*-poly( $\epsilon$ -caprolactone) (PHEMA-*g*-PCL) brush copolymers were controllable, and the molecular weight distributions were in the range of 1.28–1.32. The coupling reaction efficiency of hydroxyl-terminated mPEO (mPEO-OH) with PCL-OH in the PHEMA-*g*-PCL to produce poly(2-hydroxyethyl methacrylate)-*graft*-poly( $\epsilon$ -caprolactone)-*block*-poly(ethylene oxide) (PHEMA-*g*-(PCL-*b*-PEO)) ranged from 85.2% to 94.3%. The investigation of the melting and crystallization demonstrated that the values of crystallization temperature ( $T_c$ ), melting temperature ( $T_m$ ), and the degree of crystallinity ( $X_c$ ) of PHEMA-*g*-PCL were enhanced with the chain length increase of PCL. As for PHEMA-*g*-(PCL-*b*-PEO) brush copolymer, the  $T_m$  and  $X_c$  of the PCL blocks decreased with the chain length increase of PEO blocks. At the same time, the crystallizability of PEO segments was influenced by the brush structure of the copolymer and the PCL segments in the copolymer. Furthermore, PHEMA-*g*-PCL and PHEMA-*g*-(PCL-*b*-PEO) brush copolymers showed crystalline morphologies that were different from that of linear PCL according to the polarized optical micrographs and AFM images. Moreover, the hydrophilicity of copolymers could be improved and adjusted by the brush structure and the alteration of relative content of the PEO and PCL segments in the copolymers.

## Introduction

Branch copolymers with different architectures have attracted considerable attention over the past decade not only due to their importance in understanding the relationship of architectures with properties, but also due to their potential applications.<sup>1–6</sup> Brush copolymers are a special class of graft copolymers, in which side chains are distributed densely on a polymer backbone, and, due to their crowding arrangement, those side chains are stretched away from the backbone to form a brushlike conformation.<sup>7–15</sup> In general, three strategies including grafting-through, grafting-onto, and grafting-from have been applied in the synthesis of brush copolymers. The grafting-through method is to prepare brush copolymer via polymerization of macromonomers.<sup>16–18</sup> Yet the kinds of macromonomers used in the synthesis of brush copolymer are limited. In the grafting-onto strategy, the well-defined polymer chains are grafted onto a polymer backbone via coupling reactions.<sup>19,20</sup> Low grafting efficiency is a drawback of this synthetic strategy. In the grafting-from technique, pendant initiating groups on the backbone initiate polymerization of the monomer to form side chains.<sup>21–27</sup> Controllable/“living” polymerizations, such as atom transfer radical polymerization (ATRP)<sup>28–32</sup> and ring-opening polymerization (ROP),<sup>33</sup> are often used to prepare a number of

brush copolymers with well-defined side chains through this strategy.

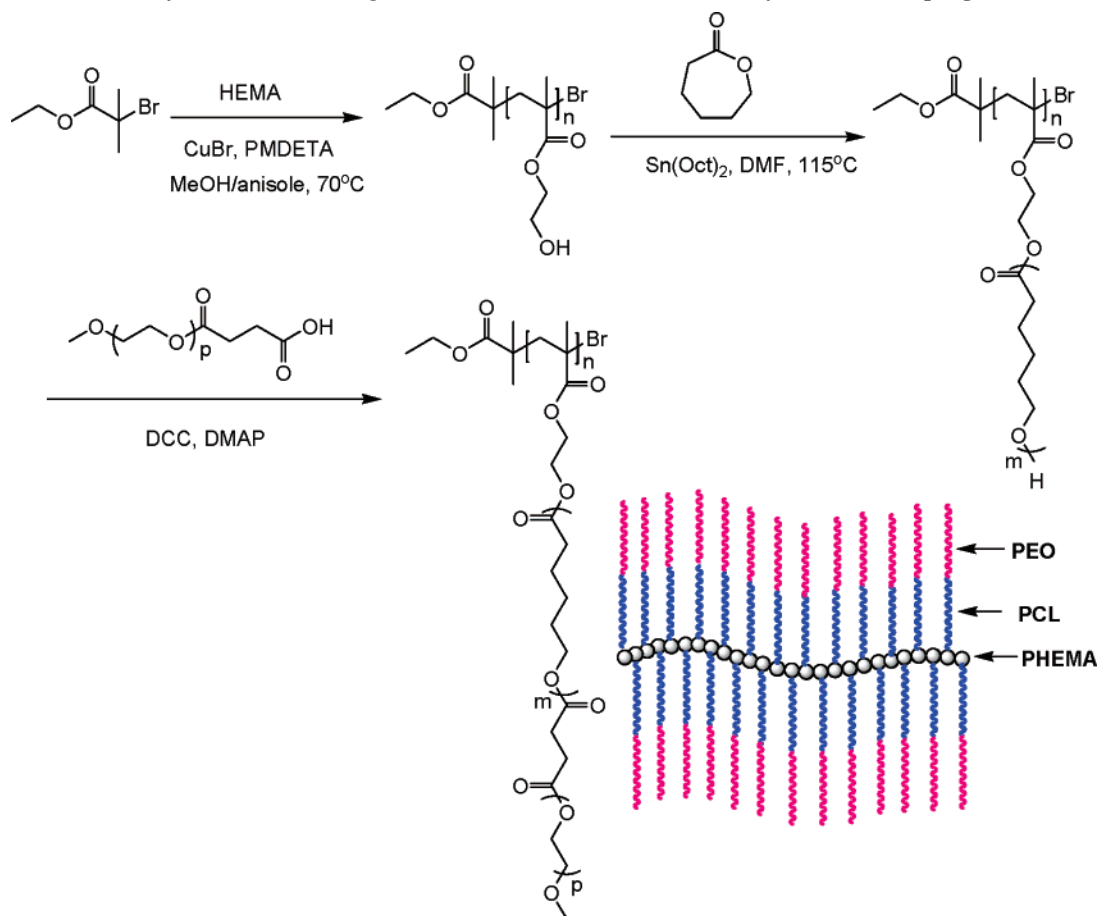
Up to now, a series of well-defined brush copolymers with various architectures have been synthesized successfully. Only a few brush copolymers with nonlinear polymers as side chain have been prepared,<sup>34–36</sup> most of the brush copolymers reported are composed of linear polymers attached onto a polymer backbone.<sup>37–41</sup> One type of those brush copolymers is attachment of two or more different linear branches on the polymer backbone; a convenient synthetic method is free radical copolymerization of binary macromonomers.<sup>38,42</sup> Another type is one linear branch distributed on the polymer backbone, and all three aforementioned synthetic strategies have been used in the synthesis of such brush copolymers.<sup>39–41,43,44</sup> In those copolymers, most of the linear homopolymers were used as side chains, such as PEO,<sup>45–48</sup> polystyrene,<sup>44–46</sup> poly(L-lactide),<sup>50</sup> poly( $\epsilon$ -caprolactone),<sup>51</sup> poly(propylene),<sup>52</sup> and polymethacrylates.<sup>32,35</sup> Only a few papers reported the applications of linear block copolymers as branch chains,<sup>38,39,41</sup> such as poly(*tert*-butyl acrylate) (or acrylic acid)-*b*-poly(*n*-butyl acrylate)<sup>39</sup> and poly(styrene)-*b*-poly(*tert*-butyl acrylate) (or acrylic acid)<sup>41</sup> prepared by successive ATRPs (following the hydrolysis of *tert*-butyl acrylate). In general, these copolymers displayed order microphases, which are formed by local segregation of dissimilar, covalently linked polymeric segments to form periodic structures. The morphology and consequently the properties of the copolymers are affected by their compositions and structures. So far, there is no report on the synthesis and properties of brush copolymers with double crystallizable side chains. Poly( $\epsilon$ -

\* Corresponding author. Tel.: +86 10 6278 3668. Fax: +86 10 6277 1149. E-mail: yuanjy@mails.tsinghua.edu.cn.

<sup>†</sup> Department of Chemistry, Tsinghua University.

<sup>‡</sup> Department of Chemical Engineering, Tsinghua University.

<sup>§</sup> University of Science and Technology of China.

Scheme 1. Synthesis of PHEMA-*g*-(PCL-*b*-PEO) Brush Macromolecule by ROP and Coupling Reaction

caprolactone) (PCL) and poly(ethylene oxide) (PEO) have good crystallizability.<sup>53,54</sup> High degree of crystallinity and hydrophobicity of biodegradable PCL limit its applications in biomedical and environment-friendly fields.<sup>55–57</sup> PEO processes good biocompatibility, hydrophilicity, and low protein absorption.<sup>58–63</sup> The brush copolymers with diblock copolymer of PCL and PEO as side chains deserve to be investigated because they are expected to display unique physical and chemical properties due to their unique double crystallizable side chain structure.

This Article presents the preparation of novel brush copolymers, poly(2-hydroxyethyl methacrylate)-*graft*-poly( $\epsilon$ -caprolactone-*b*-ethylene oxide) (PHEMA-*g*-(PCL-*b*-PEO)), with a diblock copolymer consisting of crystallizable PCL and PEO via a combination of ATRP, ROP, and coupling reaction (Scheme 1). The crystalline properties of these brush copolymers were investigated by differential scanning calorimetric analysis (DSC) and wide-angle X-ray diffraction (WAXD). The crystalline morphologies of the brush copolymers were observed by polarized optical microscopy (POM) and atomic force microscopy (AFM). The hydrophilicity of the brush copolymers was evaluated with static water contact angles.

## Experimental Section

**Materials.** 2-Hydroxyethyl methacrylate (HEMA; Acros Organic, USA) was treated by passing through a column of alumina for removal of inhibitor and then was distilled in a vacuum.  $\epsilon$ -Caprolactone (Acros Organic, USA) was distilled under reduced pressure after being treated with  $\text{CaH}_2$ . Ethyl 2-bromoisobutyrate (Aldrich, USA) was used as received. Pentamethyldiethylenetriamine (PMDETA; Acros Organic, USA) was stirred overnight over  $\text{CaH}_2$  and distilled under reduced pressure prior to use.  $\text{CuBr}$  was purified by stirring in acetic acid and washing with ethanol, and

then dried in a vacuum. Tin 2-ethylhexanoate ( $\text{Sn}(\text{Oct})_2$ ; Aldrich, USA) was distilled under reduced pressure before use. Methoxy poly(ethylene glycol)s with  $M_n = 750, 1.1\text{K}, 2\text{K},$  and  $5\text{K}$ , denoted as mPEO750, mPEO1.1K, mPEO2K, and mPEO5K, respectively (Fluka, USA), were dried by azeotropic distillation in the presence of toluene. Dicyclohexylcarbodiimide (DCC; Alfa Aesar, USA) and 4-dimethylaminopyridine (DMAP; Fluka, USA) were used as received. Succinic anhydride (Fluka, USA) was crystallized from acetic anhydride. Methanol was dried with molecular sieves type 4A before use. Methylene chloride, chloroform, triethylamine, anisole, 1,4-dioxane, tetrahydrofuran (THF), and *N,N*-dimethylformamide (DMF) were dried over  $\text{CaH}_2$  and distilled before use.

**Characterization.** Fourier transform infrared (FT-IR) spectra were recorded on an AVATAR 360 ESP FT-IR spectrometer.  $^1\text{H}$  NMR and  $^{13}\text{C}$  NMR spectra were obtained from a JEOL JNM-ECA300 NMR spectrometer with  $\text{CDCl}_3$  or  $\text{DMSO}-d_6$  as a solvent. The chemical shifts were relative to tetramethylsilane. The molecular weight and molecular weight distribution were measured on a PE Series 200 gel permeation chromatograph (Perkin-Elmer, USA). DMF was used as eluent at a flow rate of 1 mL/min at 25 °C. Narrowed poly(methyl methacrylate)s were used as calibration standard. The molecular weight and molecular weight distribution of brush copolymers were measured on a Viscotek TDA 302 gel permeation chromatograph equipped with two columns (GMHHR-H, M Mixed Bed). THF was used as eluent at a flow rate of 1 mL/min at 30 °C. DSC was carried on a DSC TA-60WS thermal analysis system (Shimadzu, Japan). Samples were first heated from  $-20$  to  $100$  °C at a heating rate of  $10$  °C/min under nitrogen atmosphere, followed by cooling to  $-20$  °C at  $10$  °C/min after stopping at  $100$  °C for 3 min, and finally heating to  $100$  °C at  $10$  °C/min. WAXD patterns of powder samples were obtained at room temperature on a  $\text{Cu K}\alpha$  radiation source using a Bruker AXS D8 Advance X-ray diffractometer (Bruker, Germany). The supplied voltage and current were set to 40 kV and 120 mA. Samples were

exposed at a scanning rate of  $2\theta = 4^\circ/\text{min}$  between  $2\theta$  values from  $1.5^\circ$  to  $60^\circ$ . The crystalline morphology of the polymer was observed using a XS-402 polarized optical microscope (Shanghai Microimage Technology, China). The samples were prepared by spin-coating of polymer solution in chloroform (15 mg/mL) on a glass plate at room temperature and then were placed at room temperature for 24 h for complete evaporation of the solvent. The AFM images of the polymers were recorded on a SPM-9500J3 atomic force microscope (Shimadzu, Japan). The films with thickness of  $\sim 280$  nm were obtained by spin-coating of polymer solution (15 mg/mL) on transparent mica. The measurements of static contact angles were carried out by commercial instruments (OCA 20, DataPhysics Instruments GmbH, Filderstadt). A distilled water droplet of  $2 \mu\text{L}$  was used as the indicator.

**Synthesis of PHEMA.** A dry Schlenk flask with a magnetic stirrer was charged with CuBr (44.6 mg, 0.31 mmol), ethyl 2-bromoisobutyrate (60.7 mg, 0.31 mmol), HEMA (8.1 g, 62.24 mmol), and solvent (65/35 v/v anisole/methanol, 8 mL). The flask was degassed with three freeze–evacuate–thaw cycles. PMDETA (65  $\mu\text{L}$ , 0.31 mmol) was deoxygenated by bubbling dry nitrogen before injection into the reaction system by syringe. Next, the polymerization was performed at  $70^\circ\text{C}$  for 5 h. After being cooled to room temperature, the reaction flask was open to air, and the crude product was dissolved in methanol and passed through an oxide alumina column to remove the copper catalysts. The polymer was obtained by precipitation in THF and dried in vacuo for 48 h.

$M_{n,\text{GPC}} = 10\,900$ ,  $M_w/M_n = 1.38$ . IR (KBr,  $\text{cm}^{-1}$ ): 3070–3722 ( $\nu_{\text{O-H}}$ ), 2948 ( $\nu_{\text{C-H}}$ ), 2884 ( $\nu_{\text{C-H}}$ ), 1724 ( $\nu_{\text{C=O}}$ ).  $^1\text{H}$  NMR (DMSO- $d_6$ ,  $\delta$ , ppm): 4.75 (s, OH), 3.86 (m,  $\text{COOCH}_2$ ), 3.54 (m,  $\text{CH}_2\text{OH}$ ), 1.61–2.03 (m,  $\text{CH}_2$ ), 0.61–1.06 (m,  $\text{CH}_3$ ).

**Synthesis of PHEMA-g-PCL Copolymer.** A typical polymerization procedure was as follows. The PHEMA ( $M_n = 10\,900$ , 0.396 g, 36.33  $\mu\text{mol}$ ) was dissolved in 2 mL of freshly distilled anhydrous DMF in a fire-dried polymerization tube. CL (6.8 g, 59.58 mmol),  $\text{Sn}(\text{Oct})_2$  (24.1 mg,  $5.96 \times 10^{-2}$  mmol), and a dried magnetic stirring bar were added into the polymerization tube. The tube was then connected to a Schlenk line, where exhausting–refilling processes were repeated three times. The tube was immersed into an oil bath at  $115^\circ\text{C}$  under nitrogen atmosphere with vigorous stirring for 24 h. After being cooled to room temperature, the resultant polymer was dissolved in chloroform and precipitated twice from methanol, affording the purified graft copolymer. The purified copolymer was dried in a vacuum oven until constant weight.

$M_{n,\text{GPC}} = 157\,600$ ,  $M_w/M_n = 1.28$ . IR (KBr,  $\text{cm}^{-1}$ ): 3412–3610 ( $\nu_{\text{O-H}}$ ), 2946 ( $\nu_{\text{C-H}}$ ), 2866 ( $\nu_{\text{C-H}}$ ), 1730 ( $\nu_{\text{C=O}}$ ).  $^1\text{H}$  NMR ( $\text{CDCl}_3$ ,  $\delta$ , ppm): 4.05 (m,  $\text{CH}_2\text{CH}_2\text{CH}_2\text{CH}_2\text{CH}_2\text{OCO}$  in PCL), 3.63 (t,  $\text{OCOCH}_2\text{CH}_2\text{CH}_2\text{CH}_2\text{CH}_2\text{OH}$  in PCL), 2.30 (m,  $\text{CH}_2\text{CH}_2\text{CH}_2\text{CH}_2\text{CH}_2\text{OCO}$  in PCL), 1.64 (m,  $\text{CH}_2\text{CH}_2\text{CH}_2\text{CH}_2\text{CH}_2\text{OCO}$  in PCL), 1.38 (m,  $\text{CH}_2\text{CH}_2\text{CH}_2\text{CH}_2\text{CH}_2\text{OCO}$  in PCL).  $^{13}\text{C}$  NMR ( $\text{CDCl}_3$ ,  $\delta$ , ppm): 173.7 ( $\text{CH}_2\text{CH}_2\text{CH}_2\text{CH}_2\text{CH}_2\text{OCO}$  in PCL), 64.3 ( $\text{CH}_2\text{CH}_2\text{CH}_2\text{CH}_2\text{CH}_2\text{OCO}$  in PCL), 34.1 ( $\text{CH}_2\text{CH}_2\text{CH}_2\text{CH}_2\text{CH}_2\text{OCO}$  in PCL), 28.2 ( $\text{CH}_2\text{CH}_2\text{CH}_2\text{CH}_2\text{CH}_2\text{OCO}$  in PCL), 25.6 ( $\text{CH}_2\text{CH}_2\text{CH}_2\text{CH}_2\text{CH}_2\text{OCO}$  in PCL), 24.6 ( $\text{CH}_2\text{CH}_2\text{CH}_2\text{CH}_2\text{CH}_2\text{OCO}$  in PCL).

**Synthesis of Carboxyl-Terminated mPEOs (mPEO-COOH).** A typical example is given below. The mPEO5K (5.2 g, 1.04 mmol), succinic anhydride (156 mg, 1.56 mmol), DMAP (127 mg, 1.04 mmol), and triethylamine (105 mg, 1.04 mmol) were dissolved in 40 mL of anhydrous 1,4-dioxane, and the reaction was carried out at room temperature for 24 h under vigorous stirring. The residue was dissolved in methylene chloride and was precipitated in diethyl ether. The purified product was dried in vacuo until constant weight.

IR (KBr,  $\text{cm}^{-1}$ ): 2884 ( $\nu_{\text{C-H}}$ ), 1730 ( $\nu_{\text{C=O}}$ ), 1645 ( $\nu_{\text{C=O}}$ ).  $^1\text{H}$  NMR ( $\text{CDCl}_3$ ,  $\delta$ , ppm): 4.25 (t,  $\text{COOCH}_2$ ), 3.65 (m,  $\text{OCH}_2\text{CH}_2\text{O}$ ), 3.38 (s,  $\text{CH}_3\text{O}$ ), 2.60 (m,  $\text{OCOCH}_2\text{CH}_2\text{OCO}$ ).

**Synthesis of PHEMA-g-(PCL-*b*-PEO) Copolymer.** A typical example was as follows. The PHEMA-g-PCL2 ( $M_n = 157\,600$ , 1.02 g, 6.47  $\mu\text{mol}$ ), mPEO5K-COOH (2.841 g, 0.557 mmol), DCC (140.3 mg, 0.68 mmol), and DMAP (36.6 mg, 0.3 mmol) were

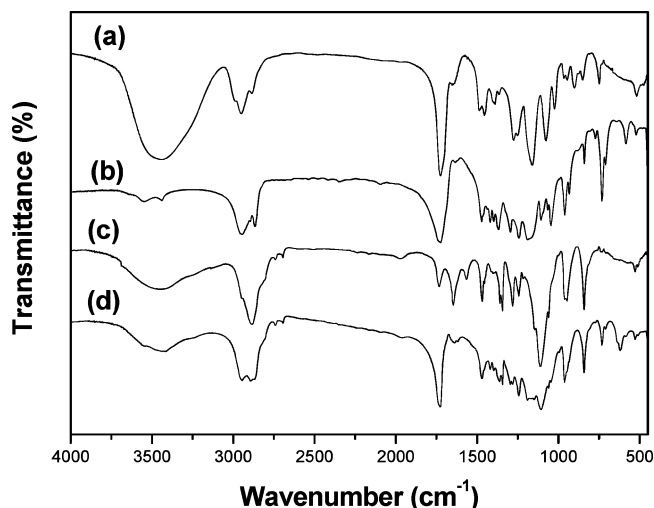


**Figure 1.** FT-IR spectra of (a) PHEMA, (b) PHEMA-g-PCL2, (c) mPEO2K-COOH, and (d) PHEMA-g-PCL2-*b*-PEO2K.

dissolved in 20 mL of anhydrous methylene chloride, and the reaction was performed at room temperature for 24 h under nitrogen atmosphere. The reaction byproduct dicyclohexylcarbodiurea was removed by filtration, and the filtered solution was evaporated to dryness. The solid was dissolved in chloroform, and the solution was extracted with a diluted HCl solution (pH = 5.0), followed by water, and then dried over anhydrous  $\text{Na}_2\text{SO}_4$ . After evaporation of solvent, the resultant product was purified by precipitating from diethyl ether.

$M_{n,\text{NMR}} = 536\,500$ . IR (KBr,  $\text{cm}^{-1}$ ): 2946 ( $\nu_{\text{C-H}}$ ), 2884 ( $\nu_{\text{C-H}}$ ), 1730 ( $\nu_{\text{C=O}}$ ), 1645 ( $\nu_{\text{C=O}}$ ).  $^1\text{H}$  NMR ( $\text{CDCl}_3$ ,  $\delta$ , ppm): 4.22 (t,  $\text{COOCH}_2$  in PEO), 4.05 (m,  $\text{CH}_2\text{CH}_2\text{CH}_2\text{CH}_2\text{CH}_2\text{OCO}$  in PCL), 3.64 (m,  $\text{OCH}_2\text{CH}_2\text{O}$  in PEO), 3.37 (s,  $\text{CH}_3\text{O}$  in PEO), 2.62 (m,  $\text{OCOCH}_2\text{CH}_2\text{OCO}$  in PEO), 2.30 (m,  $\text{CH}_2\text{CH}_2\text{CH}_2\text{CH}_2\text{CH}_2\text{OCO}$  in PCL), 1.63 (m,  $\text{CH}_2\text{CH}_2\text{CH}_2\text{CH}_2\text{CH}_2\text{OCO}$  in PCL), 1.38 (m,  $\text{CH}_2\text{CH}_2\text{CH}_2\text{CH}_2\text{CH}_2\text{OCO}$  in PCL).  $^{13}\text{C}$  NMR ( $\text{CDCl}_3$ ,  $\delta$ , ppm): 173.7 ( $\text{CH}_2\text{CH}_2\text{CH}_2\text{CH}_2\text{CH}_2\text{OCO}$  in PCL), 70.6 ( $\text{CH}_2\text{CH}_2\text{O}$  in PEO), 64.3 ( $\text{CH}_2\text{CH}_2\text{CH}_2\text{CH}_2\text{CH}_2\text{OCO}$  in PCL), 34.1 ( $\text{CH}_2\text{CH}_2\text{CH}_2\text{CH}_2\text{CH}_2\text{OCO}$  in PCL), 28.5 ( $\text{CH}_2\text{CH}_2\text{CH}_2\text{CH}_2\text{CH}_2\text{OCO}$  in PCL), 25.6 ( $\text{CH}_2\text{CH}_2\text{CH}_2\text{CH}_2\text{CH}_2\text{OCO}$  in PCL), 24.6 ( $\text{CH}_2\text{CH}_2\text{CH}_2\text{CH}_2\text{CH}_2\text{OCO}$  in PCL).

## Results and Discussion

**Preparation of PHEMA-g-PCL Copolymer.** PHEMA was synthesized by ATRP at  $70^\circ\text{C}$  with the feed molar ratio of  $[\text{HEMA}]:[\text{C-Br}]:[\text{CuBr}]:[\text{PMDETA}] = 200:1:1:1$  using the ethyl 2-bromoisobutyrate as initiator. The conversion of HEMA was 42.5% after 5 h polymerization. PHEMA was characterized by FT-IR (Figure 1a),  $^1\text{H}$  NMR, and GPC.

The molecular weight ( $M_n = 10\,900$ ) and molecular weight distribution ( $M_w/M_n = 1.38$ ) of the linear macroinitiator were obtained from GPC measurements, and its number-average degree of polymerization was 82. The apparent molecular weight obtained by GPC agrees with the theoretical molecular weight calculated by monomer conversion ( $M_{n,\text{th}} = \text{conversion} \times M_{\text{HEMA}} \times [\text{HEMA}]_0/[\text{C-Br}]_0 + M_{\text{initiator}} = 11\,300$ ). The hydroxyl groups in the side chains of PHEMA could initiate the ROP of CL in DMF at  $115^\circ\text{C}$ . The DMF was employed as solvent to ensure a homogeneous polymerization because the PHEMA and PHEMA-g-PCL are soluble in DMF. The FT-IR spectrum of PHEMA-g-PCL copolymer is shown in Figure 1b. The broad absorption at  $\nu = 3412\text{--}3610 \text{ cm}^{-1}$  is ascribed to the absorption band of the hydroxyl group in PHEMA-g-PCL. In comparison with the FT-IR spectrum of PHEMA in Figure 1a, the absorption band of the hydroxyl group of PHEMA-g-PCL decreased greatly due to polymerization leading to the



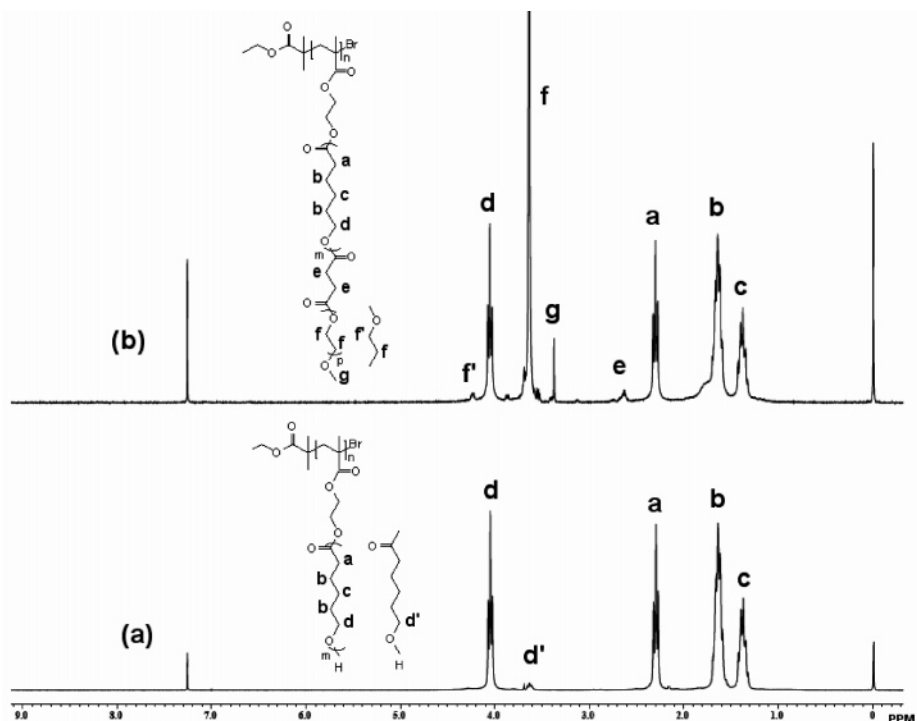


Figure 2.  $^1\text{H}$  NMR spectra of (a) PHEMA-g-PCL2 and (b) PHEMA-g-PCL2-b-PEO2K.

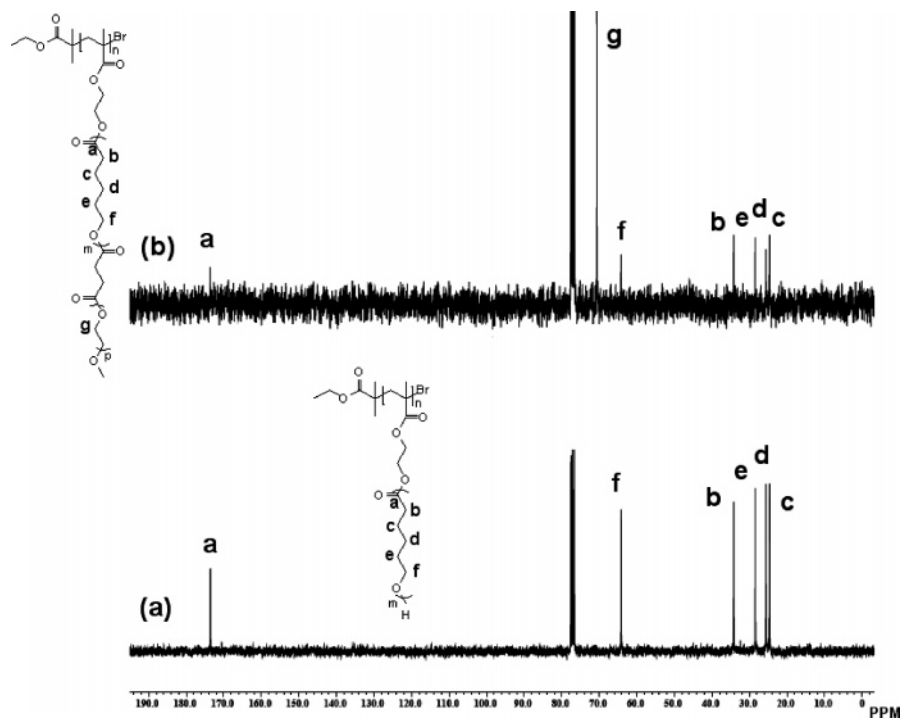


Figure 3.  $^{13}\text{C}$  NMR spectra of (a) PHEMA-g-PCL2 and (b) PHEMA-g-PCL2-b-PEO2K.

decrease of the content of hydroxyl groups in copolymer. The  $^1\text{H}$  NMR spectrum of PHEMA-g-PCL2 with assignments is shown in Figure 2a. The major resonance signals a–d are attributed to PCL. The methylene proton signal (d',  $\delta = 3.63$  ppm) indicated that PCL was terminated by hydroxyl groups.  $^{13}\text{C}$  NMR analysis was employed to investigate further the structure of the copolymer. The  $^{13}\text{C}$  NMR spectrum of PHEMA-g-PCL2 (Figure 3a) with assignment shows the typical signals of the PCL at 173.7, 64.3, 34.1, 28.2, 25.6, and 24.6 ppm.

To obtain brush copolymers with different molecular weights, the feed molar ratio of CL and hydroxyl groups of PHEMA was varied ( $[\text{CL}]/[\text{OH}] = 10, 20, 30, \text{ and } 40$ ). Assume that every

hydroxyl group of PHEMA chains took a part in initiation, the molecular weights ( $M_{n,\text{NMR}}$ ) of the resultant PHEMA-g-PCL can be calculated from the integration ratio of the methylene protons next to ether oxygen (d) to the methylene protons in the terminal hydroxyl group (d'). The results in Table 1 show that the molecular weights of the resultant PHEMA-g-PCL copolymers increased linearly with the molar ratio of monomer to initiator and the molecular weight distributions were narrow ( $M_w/M_n \leq 1.32$ ). The agreement of  $M_{n,\text{th}}$  with  $M_{n,\text{NMR}}$  indicates that the hydroxyl groups in PHEMA are effective initiating sites, and a macromolecular brush was efficiently prepared.

**Table 1. Preparation of PHEMA-g-PCL Brush Copolymers by ROP<sup>a</sup>**

sample	[CL]/[OH]	$M_{n,th}^b$	$M_{n,NMR}^c$	$M_{n,GPC}^d$	$M_w/M_n^d$	conversion (%)
linear PCL		13 300	12 600	10 800	1.36	97.3
PHEMA-g-PCL1	10	103 100	96 800	91 600	1.31	98.6
PHEMA-g-PCL2	20	191 300	180 200	157 600	1.28	96.4
PHEMA-g-PCL3	30	271 400	254 200	209 800	1.29	92.8
PHEMA-g-PCL4	40	359 800	336 900	264 000	1.32	93.2

<sup>a</sup> Reaction conditions: [CL]/[Sn(Oct)<sub>2</sub>] = 1000, polymerization time = 24 h, and polymerization temperature = 115 °C. <sup>b</sup>  $M_{n,th} = [CL]/[OH] \times M_{n,CL} \times 82 \times \text{conversion} (\%) + M_{n,PHEMA}$ , where  $M_{n,CL}$  is the molecular weight of CL and  $M_{n,PHEMA}$  is the molecular weight of PHEMA. <sup>c</sup>  $M_{n,NMR}$  was determined by <sup>1</sup>H NMR spectroscopy. <sup>d</sup>  $M_{n,GPC}$  and  $M_w/M_n$  were determined by GPC analysis with polystyrene standards. THF was used as eluent.

**Table 2. Synthesis of PHEMA-g-(PCL-*b*-PEO) Graft-Block Copolymers by Coupling Reaction<sup>a</sup>**

sample	$M_n$ of mPEO	$M_{n,NMR}^b$	coupling efficiency (%) <sup>c</sup>	PCL in copolymer (wt %) <sup>d</sup>
PHEMA-g-PCL2- <i>b</i> -PEO750	750	244 500	94.3	69.2
PHEMA-g-PCL2- <i>b</i> -PEO1.1K	1100	270 400	93.1	62.6
PHEMA-g-PCL2- <i>b</i> -PEO2K	2000	338 700	92.9	50.0
PHEMA-g-PCL2- <i>b</i> -PEO5K	5000	535 200	85.2	31.6

<sup>a</sup> Feed molar ratio of PHEMA-g-PCLOH/PEO-COOH/DCC/DMPA = 1/86/105; solvent, CH<sub>2</sub>Cl<sub>2</sub> (20 mL); room temperature, 24 h. <sup>b</sup>  $M_{n,NMR}$  is the molecular weight of PHEMA-g-(PCL-*b*-PEO) and was determined by <sup>1</sup>H NMR data. <sup>c</sup> Coupling efficiency is defined as percentage of the terminal hydroxyl groups of PCL chains reacted with mPEO-COOH and was determined by <sup>1</sup>H NMR spectroscopy. <sup>d</sup> Calculated from the ratio of  $M_{n,NMR}$  of PCL segments to that of PHEMA-g-(PCL-*b*-PEO)s.

**Table 3. Melting and Crystallization Behaviors of PHEMA-g-PCL and PHEMA-g-(PCL-*b*-PEO) Brush Copolymers**

sample	$T_c$ (°C) <sup>a</sup>		$T_m$ (°C) <sup>b</sup>		$\Delta H_m$ (J/g) <sup>c</sup>		$X_c$ (%) <sup>d</sup>	
	$T_{c,PEO}$	$T_{c,PCL}$	$T_{m,PEO}$	$T_{m,PCL}$	$\Delta H_{m,PEO}$	$\Delta H_{m,PCL}$	$X_{c,PEO}$	$X_{c,PCL}$
linear PCL		28.9		57.3		66.4		48.8
PHEMA-g-PCL1		1.5		40.9		39.8		29.2
PHEMA-g-PCL2		15.9		49.8		54.7		40.2
PHEMA-g-PCL3		21.1		54.6		56.8		41.7
PHEMA-g-PCL4		22.2		56.2		58.3		42.8
PHEMA-g-PCL2- <i>b</i> -PEO750		13.6		45.2		32.8		24.1
PHEMA-g-PCL2- <i>b</i> -PEO1.1K		12.3	28.5	44.7	41.4			
PHEMA-g-PCL2- <i>b</i> -PEO2K	25.1	20.3	53.1	43.8	63.3			
PHEMA-g-PCL2- <i>b</i> -PEO5K	29.3		58.9		75.8		35.5	
mPEO5k	37.8		59.5, 62.4		154.4		72.3	

<sup>a</sup>  $T_{c,PEO}$  and  $T_{c,PCL}$  denote the crystallization temperatures of PEO and PCL segments in the cooling run, respectively. <sup>b</sup>  $T_{m,PEO}$  and  $T_{m,PCL}$  are the melting points of PEO and PCL segments in the second heating run, respectively. <sup>c</sup>  $\Delta H_{m,PEO}$  and  $\Delta H_{m,PCL}$  denote the fusion enthalpies of PEO and PCL segments in the second heating run, respectively. <sup>d</sup>  $X_{c,PEO} = \Delta H_{m,PEO}/\Delta H_{m,PEO}^0$  and  $X_{c,PCL} = \Delta H_{m,PCL}/\Delta H_{m,PCL}^0$ , where  $\Delta H_{m,PEO}^0$  is 213.7 J/g and  $\Delta H_{m,PCL}^0$  is 136.1 J/g.

**Preparation of PHEMA-g-(PCL-*b*-PEO) Copolymer.** The mPEO-COOHs used in the following coupling reaction were synthesized by reaction of mPEO-OH with succinic anhydride. The FT-IR spectrum of mPEO2K-COOH shown in Figure 1c shows the characteristic absorption band of ester carbonyl at  $\nu = 1730$  and acid carbonyl at  $\nu = 1645$  cm<sup>-1</sup>, which indicates that mPEO-COOH was synthesized successfully. The coupling reaction of PHEMA-g-PCL-OH with a slight excess of mPEO-COOH was carried out at room temperature in the presence of DCC and DMAP. As shown in Figure 1d, the intensity of the C-H stretching band of PEO at 2884 cm<sup>-1</sup> increased and the acid carbonyl absorption band at 1645 cm<sup>-1</sup> decreased greatly, which proved that mPEO-COOH was coupled with the PCL block of PHEMA-g-PCL successfully. As compared to the <sup>1</sup>H NMR spectrum of the parent copolymer PHEMA-g-PCL in Figure 1a, new signals at  $\delta = 3.65$  and 3.38 ppm assigned to methylene and methyl protons in PEO block could be observed in Figure 2b, and the compositions of these block copolymers could be calculated from the relative integral values of the methylene protons (f) of PEO and that (a) of PCL blocks. The results are listed in Table 2.

At the same time, according to the relative integral values of the methylene protons (f) of PEO and that (a) of PCL blocks calculated from the <sup>1</sup>H NMR spectra, the coupling efficiency can be easily measured, from 85.2% to 94.3%. Figure 3b shows

the <sup>13</sup>C NMR spectrum and the assignments of carbon signals in PHEMA-g-(PCL2-*b*-PEO2K). The signals of the PCL block are similar to those of PCL in PHEMA-g-PCL, and there is only one carbonyl carbon signal of PCL ( $\delta = 173.7$  ppm). All of these results indicated that the PHEMA-g-(PCL-*b*-PEO) copolymer could be easily prepared by coupling reaction with PHEMA-g-PCL and mPEO-COOH.

**DSC and WAXD Analyses.** The melting and crystallization behaviors of PHEMA-g-PCL graft copolymers and PHEMA-g-(PCL-*b*-PEO) were investigated by DSC as shown in Figure 4 and Table 3.

The crystallization temperature ( $T_c$ ) was obtained from the cooling run, and the melting temperature ( $T_m$ ) and the degree of crystallinity ( $X_c$ ) were obtained from the second heating run. The results listed in Table 3 show that  $T_c$ ,  $T_m$ , and  $X_c$  of PHEMA-g-PCL are lower than those of linear PCL and increased with the length increase of the grafted PCL chains, which should be attributed mainly to the crystalline imperfection of the short chain length of PCL segments in the brush copolymers. Moreover, the brush structure of these polymers should make a contribution to the imperfection. For the brush block copolymers, PHEMA-g-(PCL-*b*-PEO), the melting and crystallization behaviors are relatively complicated. When the molecular weights of PEOs are 750 and 1.1K, only  $T_c$  of PCL blocks could be obviously observed in the brush block copoly-

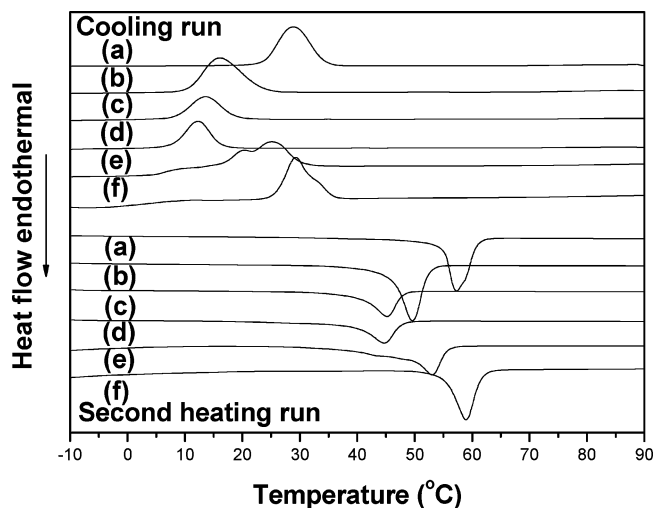


**Figure 4.** DSC curves of (a) linear PCL, (b) PHEMA-g-PCL2, (c) PHEMA-g-PCL2-*b*-PEO750, (d) PHEMA-g-(PCL2-*b*-PEO1.1K), (e) PHEMA-g-(PCL2-*b*-PEO2K), and (f) PHEMA-g-(PCL2-*b*-PEO5K) in the cooling run and the second heating run, respectively.

mers, and the values of  $T_{c,PCL}$  were lower than that of PCL in their precursor, PHEMA-g-PCL2, and decreased with the length increase of PEO blocks. However, for PHEMA-g-(PCL2-*b*-PEO2K), there are two  $T_c$ 's ( $T_{c,PCL}$  and  $T_{c,PEO}$ ) in PHEMA-g-(PCL2-*b*-PEO2K), and only a single crystallization peak assigned to PEO chains could be observed in PHEMA-g-(PCL2-*b*-PEO5K). In the second heating run of PHEMA-g-(PCL2-*b*-PEO750),  $T_m$  of PCL could be detected and was lower than that of PCL in PHEMA-g-PCL2. For PHEMA-g-(PCL2-*b*-PEO1.1K), there is a weak melting peak of PEO blocks at 28.5 °C besides an obvious melting peak of PCL blocks at 44.7 °C. The DSC curve of PHEMA-g-(PCL2-*b*-PEO2K) shows two melting peaks, but the intensity of the melting peak of PCL blocks was weaker than that of PEO blocks. From the DSC curves of PHEMA-g-(PCL2-*b*-PEO1.1K) and PHEMA-g-(PCL2-*b*-PEO2K), the individual fusion enthalpies of PCL and PEO blocks could not be calculated separately due to the partial overlapping of the melting endotherms of PCL and PEO blocks. As for PHEMA-g-(PCL2-*b*-PEO5K), only a single melting peak assigned to PEO blocks was observed.

The PEO segments in PHEMA-g-(PCL2-*b*-PEO750) cannot crystallize and are amorphous, probably because the short PEO chain is too short (PEO with less than  $M_n = 2000$  is difficult to crystallize). At the same time, the constrained geometry of the brush block copolymer and the amorphous PEO blocks together hindered the crystalline process, leading to the crystalline imperfection of the PCL segments. Similarly, the crystalline imperfection of PCL blocks in the PHEMA-g-(PCL2-*b*-PEO1.1K) should be attributed to the brush structure and the PEO segments. When the molecular weight of PEO increased to 2K, the PEO chains displayed some crystallizability. As shown in the DSC curve of PHEMA-g-(PCL2-*b*-PEO2K) in Figure 4e, in which the contents of PCL and PEO blocks are almost the same, the PCL and PEO blocks possessed crystallizability. However, the crystallizabilities of PCL and PEO segments were seriously hindered by the brush structure of the copolymer and the mutual influence between the PCL and PEO segments. Moreover, the chain conformation of brush copolymer was different from that of linear polymer. The flexibility of the chains of brush copolymer was poorer than that of the chains of linear polymer. Therefore, the chain conformation of brush copolymer resulted in less intermolecular interaction, which led

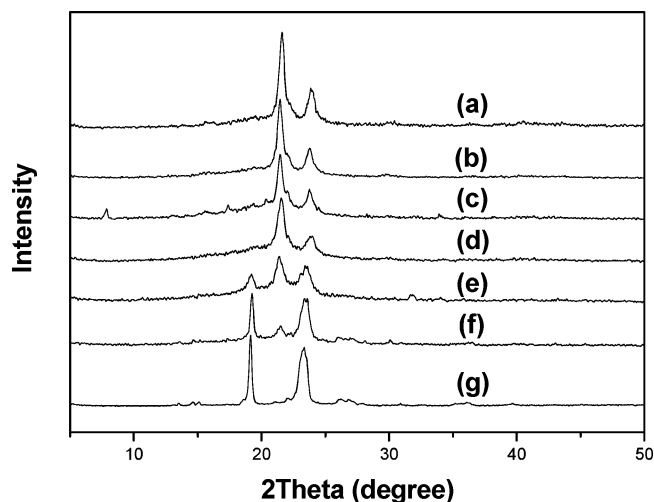


**Figure 5.** WAXD patterns of (a) linear PCL, (b) PHEMA-g-PCL2, (c) PHEMA-g-(PCL2-*b*-PEO750), (d) PHEMA-g-(PCL2-*b*-PEO1.1K), (e) PHEMA-g-(PCL2-*b*-PEO2K), (f) PHEMA-g-(PCL2-*b*-PEO5K), and (g) mPEO5K. All measurements were carried out at room temperature.

to decreasing of the enthalpy of fusion. As a result, the crystallizability of PCL and PEO segments was restrained. For the PHEMA-g-(PCL2-*b*-PEO5K) with PEO chains longer than PCL chains, the crystallizability of PCL blocks was completely hindered by the constrained geometry of the block copolymer and the PEO crystallinity. Meanwhile, the crystallizability of the PEO blocks was also affected by the macromolecular structure and the PCL chain, and its  $T_c$ ,  $T_m$ , and  $X_c$  are lower than those of mPEO5K.

WAXD is another useful method to investigate the crystal structure of the brush copolymer, PHEMA-g-PCL, and block copolymer, PHEMA-g-(PCL-*b*-PEO). Figure 5 shows WAXD patterns of linear PCL, PHEMA-g-PCL, and PHEMA-g-(PCL2-*b*-PEO). All of the samples were measured at room temperature without annealing.

Linear PCL showed intensive peaks at 21.6° and 23.9°, corresponding to the (110) and (200) planes of the orthorhombic crystal form.<sup>64,65</sup> PHEMA-g-PCL2 displayed the same crystalline structure as linear PCL according to the results in Figure 5a, which indicates that the brush structure did not change the crystalline conformation of PCL. The mPEO shows two intensive peaks at 19.1° and 23.3°.<sup>66</sup> However, PHEMA-g-(PCL2-*b*-PEO750) has only the diffraction peaks of PCL crystalline at 21.6° and 23.9°, indicating that the PEO chain presented as amorphous. In PHEMA-g-(PCL2-*b*-PEO1.1K), a weak diffraction peak at 19.1° could be observed in addition to the obvious diffraction peaks of PCL crystal, which demonstrated that PEO segments could present somewhat crystallizability. As for PHEMA-g-PCL2-*b*-PEO2K, the WAXD pattern shows reflections at 19.1°, 21.6°, and 23.3°, typical of PCL and PEO crystalline phases. The reflections of the PHEMA-g-(PCL2-*b*-PEO5K) WAXD pattern in Figure 5f are similar to those of the PHEMA-g-(PCL2-*b*-PEO2K) WAXD pattern in Figure 5e except the intensity of diffraction peaks of PEO crystalline is stronger than that of PCL crystalline. The WAXD patterns for PHEMA-g-(PCL2-*b*-PEO2K) and PHEMA-g-(PCL2-*b*-PEO5K) are almost the summation of those for the PEO and PCL homopolymers, suggesting that the PEO and PCL blocks formed separate crystal microdomains before annealing.

**Crystalline Morphologies of Polymers.** The crystalline morphologies of mPEO5K, mPEO2K, linear PCL, PHEMA-g-PCL2, PHEMA-g-(PCL2-*b*-PEO2K), and PHEMA-g-(PCL2-



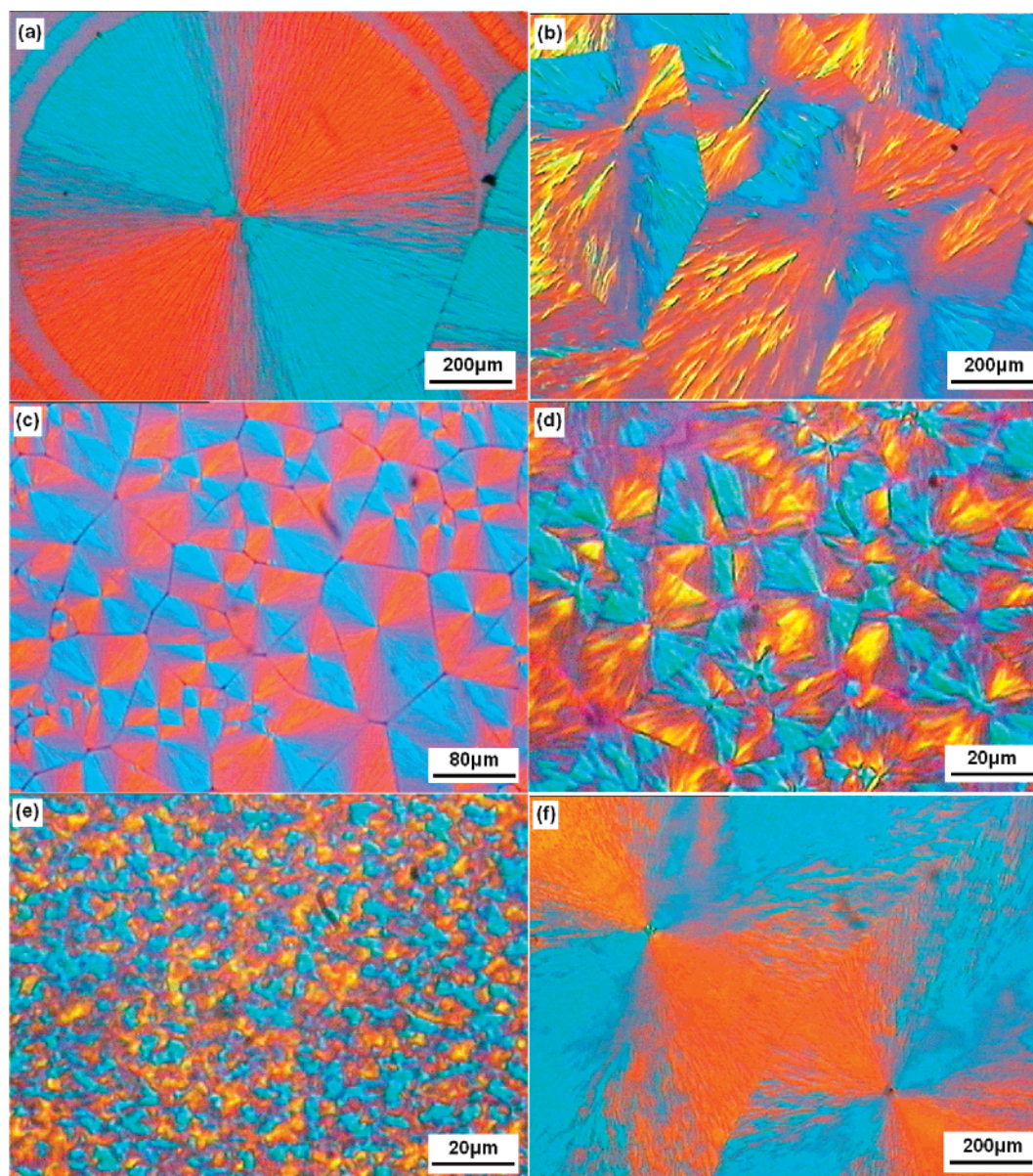


**Figure 6.** Polarized optical micrographs of (a) mPEO5K, (b) mPEO2K, (c) linear PCL, (d) PHEMA-g-PCL2, (e) PHEMA-g-(PCL2-*b*-PEO2K), and (f) PHEMA-g-(PCL2-*b*-PEO5K).

*b*-PEO5K) were investigated by polarized optical micrographs. According to Figure 6, mPEO5K showed a typical large spherulitic morphology, and Maltese cross patterns were observed. Similarly, large spherulitic morphology of mPEO2K was also observed. This indicated that mPEO homopolymers have strong crystallizability. As shown in Figure 6c, linear PCL showed a typical spherulitic morphology, but the size of the spherulites was smaller than that of mPEO. As for PHEMA-g-PCL2 brush copolymer, the size of the spherulites was much smaller than that of linear PCL, and no obvious Maltese cross patterns were found. The result could be attributed to the brush structure of copolymer and the presence of PHEMA chain in the copolymer interfering with the natural growth of the spherulites. The crystalline morphology of PHEMA-g-(PCL2-*b*-PEO2K) was different from those of mPEO2K and PHEMA-g-PCL2. Many small crystals were observed. Because of the brush structure of the copolymer and the serious mutual influence between the PEO and PCL segments, the movement ability of the chains of PCL or PEO segments decreased and the nucleation ability increased; therefore, the formation of large spherulites was impossible, and only many small crystals could

be formed. In PHEMA-g-(PCL2-*b*-PEO5K), the spherulitic morphology was obvious and the spherulites were large, which indicated that the crystallizability of PEO blocks was dominative in copolymer.

AFM images were used to confirm further the different crystalline morphologies of polymers with different structure and composition. The AFM height images of linear PCL, PHEMA-g-PCL2, and PHEMA-g-(PCL2-*b*-PEO2K) are shown in Figure 7. As shown in Figure 7a, the spherulites were relatively large for linear PCL, which indicated that linear PCL possessed good crystallizability. According to the image of PHEMA-g-PCL2 (Figure 7b), the spherulites were relatively smaller than those of linear PCL, which could be ascribed to the brush structure and the PHEMA backbone inducing the decrease of the crystallizability of copolymer. In comparison with the morphology of PHEMA-g-PCL2 shown in Figure 7b, the spherulites of PHEMA-g-(PCL2-*b*-PEO2K) in Figure 7c were tiny, which could be attributed to the mutual influence of PCL and PEO blocks leading to further weakening of the crystallizability.



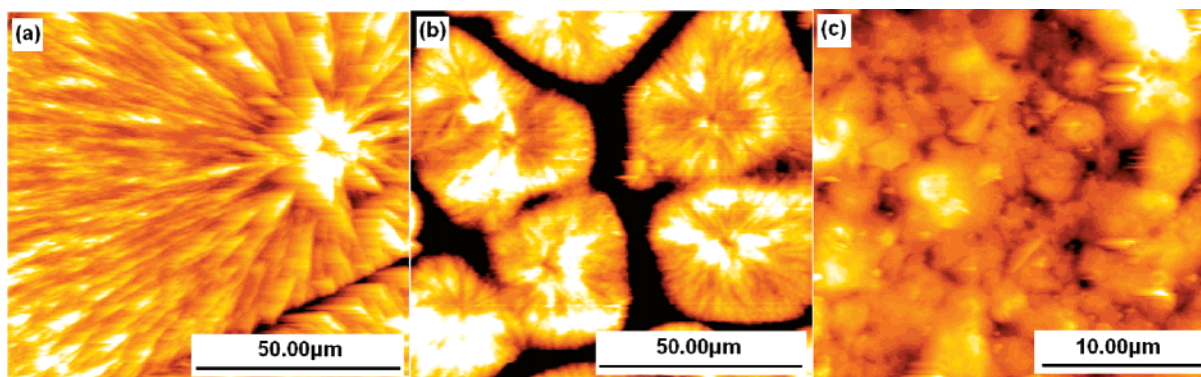


Figure 7. AFM height images of (a) linear PCL, (b) PHEMA-g-PCL2, and (c) PHEMA-g-(PCL2-*b*-PEO2K).

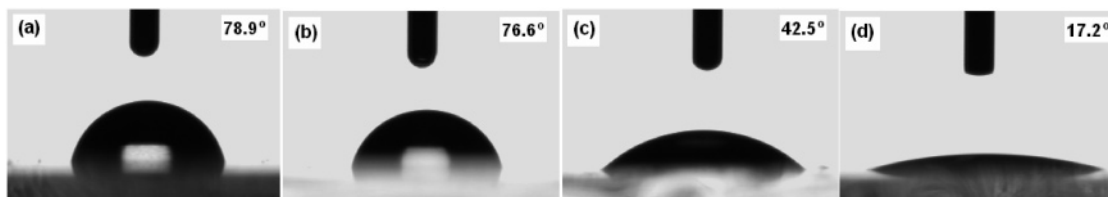


Figure 8. Photograph of the water contact angles of (a) linear PCL, (b) PHEMA-g-PCL2, (c) PHEMA-g-(PCL2-*b*-PEO2K), and (d) PHEMA-g-(PCL2-*b*-PEO5K).

**Hydrophilicity Investigation of Polymers.** The hydrophilicity of the films prepared from linear PCL, PHEMA-g-PCL2, PHEMA-g-(PCL2-*b*-PEO2K), and PHEMA-g-(PCL2-*b*-PEO5K) was measured with water contact angles. As shown in Figure 8a, the contact angle of the linear PCL surface was 78.9°. The contact angle of the PHEMA-g-PCL2 surface decreased to 76.6°, which should be ascribed to the brush structure of the copolymer and the terminal hydroxyl groups of the copolymer. As for the surfaces of PHEMA-g-(PCL2-*b*-PEO2K) and PHEMA-g-(PCL2-*b*-PEO5K), the contact angles were 42.5° and 17.2°, respectively. This should be attributed to the presence of PEO blocks with good hydrophilicity. Therefore, the hydrophilicity of copolymers could be improved and adjusted by the brush structure and the alteration of the composition of the PEO and PCL segments in copolymers.

## Conclusions

Brush copolymers with block copolymer, PCL-*b*-PEO, as side chains were synthesized successively via a combination of ROP and coupling reaction. The PHEMA backbone was prepared by ATRP, and its pendant hydroxyl groups were used as macroinitiators for ROP of CL to obtain PHEMA-g-PCL brush copolymers. The PHEMA-g-(PCL-*b*-PEO) brush copolymers were synthesized by coupling reaction of the hydroxyl-terminated PHEMA-g-PCL and carboxyl-terminated mPEO macromer. The values of  $T_c$ ,  $T_m$ , and  $X_c$  of PHEMA-g-PCL were enhanced with the chain length increase of PCL. The  $T_m$  and  $X_c$  of the PCL blocks in the PHEMA-g-(PCL-*b*-PEO) decreased with the chain length increase of the PEO blocks. The crystallizability of PEO segments is influenced by the brush structure of the copolymer and the PCL segments in the copolymer. Furthermore, PHEMA-g-PCL and PHEMA-g-(PCL-*b*-PEO) revealed crystalline morphologies different from that of linear PCL, according to the polarized optical micrographs and AFM images. The hydrophilicity of copolymers could be improved and adjusted by the brush structure and the alteration of the composition of the PEO and PCL segments in copolymers. The self-assembly behavior of the brush copolymers and their potential applications in drug delivery system will be investigated further.

**Acknowledgment.** We gratefully acknowledge the financial support of the National Natural Science Foundation of China (nos. 50373023, 20574042, and 20674044).

## References and Notes

- (1) Sheiko, S. S.; Sun Frank, C.; Randall, A.; Shirvanyants, D.; Rubinstein, M.; Lee, H.-i.; Matyjaszewski, K. *Nature (London)* **2006**, *440*, 191–194.
- (2) Sumerlin, B. S.; Neugebauer, D.; Matyjaszewski, K. *Macromolecules* **2005**, *38*, 702–708.
- (3) Neugebauer, D.; Sumerlin, B. S.; Matyjaszewski, K.; Goodhart, B.; Sheiko, S. S. *Polymer* **2004**, *45*, 8173–8179.
- (4) Dziezok, P.; Sheiko, S. S.; Fischer, K.; Schmidt, M.; Moeller, M. *Angew. Chem.* **1997**, *36*, 2812–2815.
- (5) Sheiko, S. S.; Moeller, M. *Chem. Rev.* **2001**, *101*, 4099–4123.
- (6) Lin, J. J.; Chen, I. J.; Chen, C. N.; Kwan, C. C. *Ind. Eng. Chem. Res.* **2000**, *39*, 65–71.
- (7) Fischer, K.; Schmidt, M. *Macromol. Rapid Commun.* **2001**, *22*, 787–791.
- (8) Zhang, M.; Mueller, A. H. E. *J. Polym. Sci., Part A: Polym. Chem.* **2005**, *43*, 3461–3481.
- (9) Matyjaszewski, K.; Xia, J. *Chem. Rev.* **2001**, *101*, 2921–2990.
- (10) Sun, F.; Sheiko, S. S.; Moeller, M.; Beers, K.; Matyjaszewski, K. *J. Phys. Chem. A* **2004**, *108*, 9682–9686.
- (11) Zhang, B.; Zhang, S. J.; Okrasa, L.; Pakula, T.; Stephan, T.; Schmidt, M. *Polymer* **2004**, *45*, 4009–4015.
- (12) Nakamura, Y.; Wan, Y. N.; Mays, J. W.; Iatrou, H.; Hadjichristidis, N. *Macromolecules* **2000**, *33*, 8323–8328.
- (13) He, L. H.; Huang, J.; Chen, Y. M.; Liu, L. P. *Macromolecules* **2005**, *38*, 3351–3355.
- (14) Zhang, Z. B.; Shi, Z. Q.; Han, X.; Holdcroft, S. *Macromolecules* **2007**, *40*, 2295–2298.
- (15) Zamurovic, M.; Christodoulou, S.; Vazaios, A.; Iatrou, E.; Pitsikalis, M.; Hadjichristidis, N. *Macromolecules* **2007**, *40*, 5835–5849.
- (16) Djalali, R.; Hugenberg, N.; Fischer, K.; Schmidt, M. *Macromol. Rapid Commun.* **1999**, *20*, 444–449.
- (17) Heroguez, V.; Gnanou, Y.; Fontanille, M. *Macromolecules* **1997**, *30*, 4791–4798.
- (18) Gu, L. N.; Shen, Z.; Lu, G. L.; Zhang, X. H.; Huang, X. Y. *Macromolecules* **2007**, *40*, 4486–4493.
- (19) Deffieux, A.; Schappacher, M. *Macromolecules* **1999**, *32*, 1797–1802.
- (20) Schappacher, M.; Billaud, C.; Paulo, C.; Deffieux, A. *Macromol. Chem. Phys.* **1999**, *200*, 2377–2386.
- (21) Kotani, Y.; Kato, M.; Kamigaito, M.; Sawamoto, M. *Macromolecules* **1996**, *29*, 6979–6982.
- (22) Beers, K. L.; Gaynor, S. G.; Matyjaszewski, K.; Sheiko, S. S.; Moeller, M. *Macromolecules* **1998**, *31*, 9413–9415.
- (23) Schappacher, M.; Deffieux, A.; Putaux, J.-L.; Viville, P.; Lazzaroni, R. *Macromolecules* **2003**, *36*, 5776–5783.

- (24) Neugebauer, D.; Zhang, Y.; Pakula, T.; Sheiko, S. S.; Matyjaszewski, K. *Macromolecules* **2003**, *36*, 6746–6755.
- (25) Yuan, W. Z.; Yuan, J. Y.; Zhou, M.; Sui, X. F. *J. Polym. Sci., Part A: Polym. Chem.* **2006**, *44*, 6575–6586.
- (26) He, L. H.; Zhang, Y. H.; Ren, L. X.; Chen, Y. M.; Wei, H.; Wang, D. *J. Macromol. Chem. Phys.* **2006**, *207*, 684–693.
- (27) Pietrasik, J.; Sumerlin, B. S.; Lee, R. Y.; Matyjaszewski, K. *Macromol. Chem. Phys.* **2007**, *208*, 30–36.
- (28) Mecerreyes, D.; Jerome, R.; Dubois, P. *Adv. Polym. Sci.* **1999**, *147*, 1–59.
- (29) Stridsberg, K. M.; Ryner, M.; Albertsson, A.-C. *Adv. Polym. Sci.* **2002**, *157*, 41–65.
- (30) Hashimoto, K. *Prog. Polym. Sci.* **2000**, *25*, 1411–1462.
- (31) Wang, J. S.; Matyjaszewski, K. *J. Am. Chem. Soc.* **1995**, *117*, 5614–5615.
- (32) Kato, M.; Kamigaito, M.; Sawamoto, M.; Higashimura, T. *Macromolecules* **1995**, *28*, 1721–1723.
- (33) Lee, H.-i.; Jakubowski, W.; Matyjaszewski, K.; Yu, S.; Sheiko, S. S. *Macromolecules* **2006**, *39* 4983–4989.
- (34) Hirao, A.; Kawano, H.; Ryu, S. W. *Polym. Adv. Technol.* **2002**, *13*, 275–284.
- (35) Gibanel, S.; Forcada, J.; Heroguez, V.; Schappacher, M.; Gnanou, Y. *Macromolecules* **2001**, *34*, 4451–4458.
- (36) Luan, B.; Zhang, B. Q.; Pan, C. Y. *J. Polym. Sci., Part A: Polym. Chem.* **2006**, *44*, 549–560.
- (37) Lord, S. J.; Sheiko, S. S.; LaRue, I.; Lee, H.-I.; Matyjaszewski, K. *Macromolecules* **2004**, *37*, 4235–4240.
- (38) Neugebauer, D.; Theis, M.; Pakula, T.; Wegner, G.; Matyjaszewski, K. *Macromolecules* **2006**, *39*, 584–593.
- (39) Zhang, M.; Breiner, T.; Mori, H.; Muller, A. H. E. *Polymer* **2003**, *44*, 1449–1458.
- (40) Jin, L.; Liu, P.; Hu, J.; Wang, C. *Polym. Int.* **2004**, *53*, 142–148.
- (41) Cheng, G.; Boeker, A.; Zhang, M.; Krausch, G.; Mueller, A. H. E. *Macromolecules* **2001**, *34*, 6883–6888.
- (42) Tsubaki, K.; Kobayashi, H.; Sato, J.; Ishizu, K. *J. Colloid Interface Sci.* **2001**, *241*, 275–279.
- (43) Tsukahara, Y.; Ohta, Y.; Senoo, K. *Polymer* **1995**, *36*, 3413–3416.
- (44) Gao, H. F.; Matyjaszewski, K. *J. Am. Chem. Soc.* **2007**, *129*, 6633–6639.
- (45) Percec, V.; Heck, J.; Tomazos, D.; Falkenberg, F.; Blackwell, H.; Unger, G. *J. Chem. Soc., Perkin Trans. 1* **1993**, *22*, 2799–2811.
- (46) Feng, Y.; Zhao, J.; Wang, Q.; Li, M.; Chen, X. *J. Appl. Polym. Sci.* **2000**, *75*, 475–479.
- (47) Li, X.; Ji, J.; Shen, J. *Macromol. Rapid Commun.* **2006**, *27*, 214–218.
- (48) Li, Y.-G.; Shi, P.-J.; Zhou, Y.; Pan, C.-Y. *Polym. Int.* **2004**, *53*, 349–354.
- (49) Li, A.; Lu, Z.; Zhou, Q.; Qiu, F.; Yang, Y. *Polymer* **2006**, *47*, 1774–1777.
- (50) Chen, H.; Chen, T.; Hu, J.; Wang, C. *Colloids Surf., A* **2005**, *268*, 24–29.
- (51) Xu, X.; Huang, J. *J. Polym. Sci., Part A: Polym. Chem.* **2006**, *44*, 467–476.
- (52) Lin, J. J.; Young, M. Y.; Shau, S. M.; Cheng, I. J. *Polymer* **2000**, *41*, 2405–2417.
- (53) Srivastava, R. K.; Albertsson, A.-C. *Macromolecules* **2006**, *39*, 46–54.
- (54) Gillies, E. R.; Frechet, J. M. J. *J. Am. Chem. Soc.* **2002**, *124*, 14137–14146.
- (55) Persenaire, O.; Alexandre, M.; Degee, P.; Dubois, P. *Biomacromolecules* **2001**, *2*, 288–294.
- (56) Cho, E. C.; Cho, K.; Ahn, J. K.; Kim, J.; Chang, I. S. *Biomacromolecules* **2006**, *7*, 1679–1685.
- (57) Lam, H. F.; Gong, X. J.; Wu, C. *J. Phys. Chem. B* **2007**, *111*, 1531–1535.
- (58) Tanaka, S.; Ogura, A.; Kaneko, T.; Murata, Y.; Akashi, M. *Biomacromolecules* **2004**, *5*, 2447–2455.
- (59) Maglio, G.; Nese, G.; Nuzzo, M.; Palumbo, R. *Macromol. Rapid Commun.* **2004**, *25*, 1139–1144.
- (60) Agrawal, S. K.; Sanabria-DeLong, N.; Jemian, P. R.; Tew, G. N.; Bhatia, S. R. *Langmuir* **2007**, *23*, 5039–5044.
- (61) Lodge, T. P.; Rasdal, A.; Li, Z. B.; Hillmyer, M. A. *J. Am. Chem. Soc.* **2005**, *127*, 17608–17609.
- (62) Feng, X. S.; Taton, D.; Borsali, R.; Chaikof, E. L.; Gnanou, Y. *J. Am. Chem. Soc.* **2006**, *128*, 11551–11562.
- (63) Pugh, C.; Bae, J. Y.; Scott, J. R.; Wilkins, C. L. *Macromolecules* **1997**, *30*, 8139–8152.
- (64) Wang, L.; Wang, J. L.; Dong, C. M. *J. Polym. Sci., Part A: Polym. Chem.* **2005**, *43*, 4721–4730.
- (65) Chen, L.; Ni, Y. S.; Bian, X. C.; Qiu, X. Y.; Zhuang, X. L.; Chen, X. S.; Jiang, X. B. *Carbohydr. Polym.* **2005**, *60*, 103–109.
- (66) Maglio, G.; Nese, G.; Nuzzo, M.; Palumbo, R. *Macromol. Rapid Commun.* **2004**, *25*, 1139–1144.

MA071841U